Higher order chemical reaction and thermal conductivity effects on Non-Newtonian Casson fluid flow over a Stretching Surface

S. ANURADHA[1] and M. PRIYA[2]

** [1] Professor & Head in Department of Mathematics, Hindusthan College of Arts & Science, Coimbatore-641028, Tamilnadu, India.E-mail:researchhmt@gmail.com.*
** [2] Research Scholar in Department of mathematics, Hindusthan College of Arts & Science, Coimbatore-641028, Tamilnadu, India, E-mail:priya.jeni28@gmail.com.*

Corresponding author: researchhmt@gmail.com

ABSTRACT

This research article presents with the 3D steady flow of Casson liquid over an extending surface. Assessment is accomplished in the context of Brownian movement, variable thermal conductivity, higher order chemical reaction and thermophoresis impacts. Similarity transformations are utilized to recreate the boundary layer PDE's into ordinary differential equations. Due to their extreme nonlinearity, these equations cannot be resolved analytically. So, it was resolved using bvp4c MATLAB solvers. Analysis and discussion are conducted on the effects of significant physical parameters on the flow velocity, temperature, and concentration profiles. Numerical values of skin friction coefficients , Nusselt and Sherwood numbers for various values of Ratio parameter , Thermophoresis parameter, Order of chemical reaction , Schmidt Number , Thermal conductivity parameter, Brownian motion, Heat absorption parameter, Chemical reaction parameter, and Prandtl Number are registered and inspected.

Keywords: 3D flow, Stretching surface, Brownian motion, Heat & Mass transfer, Casson fluid, Steady flow and Chemical reaction.

DOI: 10.48047/ecb/2023.12.8.577

1.INTRODUCTION

During the past few decades, the mass and heat transmission past an extending surface has achieved a significant response from numerous researchers for its important applications in business and chemical industries. Non-Newtonian liquids are those that do not follow Newton's law of viscosity, with Casson fluids being the most frequently seen. Multidimensional fluids, such as suspensions, sugar solutions, banana juice, delusions, vaccines, toned milk and clay coating stand out as a result of their many industrial applications.

Abdela and Shankar [1] presented a mathematical model to explore Maxwell Nanofluid stagnation point flow with non-uniform thermal radiation and heat source effects. Alreshidi et al. [2] utilized both analytical and numerical methodologies to represent the issue with the three-dimensional flow produced by a porous rotating disk along with Brownian motion (Nb) and Thermophoresis (Nt) Effects. Animasaun [3] applied the R-K Gill method to depict the characteristics of heat and mass transport on Casson fluid flow with varying viscosity and thermal conductivity. In order to account for chemical reaction, thermophoresis and Brownian motion effects, Arshad et al. [4] explored the three-dimensional Nanofluid flow across an exponentially increasing sheet using the bvp4c method. Falana et al. obtained analysis of the 2D boundary layer Nanofluid flow brought on by a permeable stretching sheet was published in [5]. Using the R-K-Fehlberg approach, Gopal and Kishan [6] discovered a mathematical representation to describe the Casson Nanofluid flow through a nonlinearly elastic sheet. Gopal et al., [7] computed Numerical solution of an electrically conducting Nanofluid flow under chemical reaction and viscous dissipation. The Casson liquid flow with chemical reaction was examined by Hari Krishna et al., [8] using the Fourth order Explicit R-K approach. Ismail et al., [9] put light on Non-Newtonian flow across a moving plate under varying thermal conductivity using Fourth order Explicit R-K method. Jana and Das [10] explored the slip flow across a flat plate with a convective surface, chemical processes and thermal radiation. Jangid et al., [11] examined the modelling of heat and mass transport processes in an extended porous wall Casson fluid flow with consequences of radiation, chemical processes and thermal diffusion. Khan et al. [12] provided a numerical illustration of Casson liquid flow across a permeable moving wedge. In order to illustrate the impacts of first order chemical processes and thermos-diffusion on three-dimensional Maxwell fluid past an expanding sheet in a porous medium channel, Kumar et al., [13] used the MATLAB bvp4c algorithm. Heat and mass transmission study of MHD Casson liquid flow through a porous Riga plate was addressed by Loganathan and Deepa [14] using the Crank-Nicholson implicit technique. Reddy et al. [15] conducted a comparative analysis of non-Newtonian fluid flow across an extended sheet together with the consequences of chemical reaction process and radiation. Utilizing Homotopy Analysis Technique, Majeed et al., [16] scrutinized the Thermophoretic and Brownian moment influence of MHD Nanofluid flow. Makinde [17] used the R-K integration technique to establish the consequence of mixed convective flow across a vertical porous plate with heat radiation and nth order chemical reaction. The double diffusive outcome of a non-linear Nano liquid flow towards an elastic sheet were numerically researched by Makkar et al., [18].By

employing the HAM method, Mittal and Patel [19] investigated the influence of heat production, radiation and thermophoresis on MHD 2D flow. Using the Spectral Quasi-Linearization (SQL) approach, Mondal et al., [20] have studied the solutions for three-dimensional Magneto hydrodynamic flow. Radha et al., [21] used bvp4c to explore how the thermophysical properties of Casson fluid flow towards an exponential stretching sheet can alter. Heat and mass transmission study of steady flow were established by Raju et al. [22]. Ramadevi et al., [23] evaluate the perturbation technique to study how heat and mass transport influenced a wrinkle surface in an unsteady flow. To examine the MHD Nanofluid flow across surface, Rasheed et al. [24] used the HAM analytical technique. Reddy et al. [25] examined Williamson nanofluid flow with variable thickness and variable thermal conductivity. Sarojamma et al. [26] have solved the MHD Maxwell fluid model while taking into account both homogeneous and heterogeneous chemical reactions as well as variable thermal conductivity. An MHD two-dimensional Casson fluid flow past a vertical channel was planned by Sarojamma et al. [27]. Senapati et al., [28] have taken Casson nanofluid flow towards an exponentially stretched sheet using numerical procedure. Sivakumar and Rushi Kumar [29] discovered a fourth order R-K integration technique for the numerical treatment of two-dimensional MHD unsteady slip flow with chemical reaction. The Nanofluid flow with slip boundary conditions and higher order chemical reaction has been numerically explored by Swain et al., [30].In their study of MHD Casson fluid flow across a linearly stretched sheet with variable viscosity and thermal conductivity, Tufail and Zaib [31] looked at the mechanisms of heat and mass transmission. Casson fluid flow was characterised by Ullah et al. [32] using the Keller-Box numerical technique.

The focus of all the investigations discussed so far has been on 2-D or 3-D flows in the presence of chemical reaction, radiation, and heat generation/absorption. Yet as far as the author is aware, no research have yet examined the effects of higher order chemical reactions, thermophoresis, and Brownian movement on the flow of 3-D non-Newtonian fluids across a stretching surface. We attempt to explore the heat and mass transfer behaviour of the 3-D Casson fluid flows over a stretched surface with higher order chemical reaction and variable thermal conductivity in this work by keeping this in mind. Using the appropriate similarity transformation, the governing equations are converted to non-linear ordinary differential equations, and the solutions are computed numerically using the bvp4c MATLAB tool. We used several sets of parameter values to examine the effects of the relevant factors, and the results were then analysed for the features of flow, heat and mass transfer.

2. MATHEMATICAL FORMULATION OF THE PROBLEM

A stretching surface makes a laminar flow of an electrically conducting and incompressible Casson fluid. The flow is restricted to $z \geq 0$.The stretching surface velocities are assumed to be U=ax, V=by, and w=0 on the xy-plane, where a and b are constants. The fluid flow is being affected normally by the constant magnetic field B0, with the induced magnetic field believed to be insignificant. The formulation of the current issue is modelled in light of the ensuing assumptions.

1. Steady, 3D, boundary layer flow.

2. Casson liquid model.

3. The consequences of chemical reactions and heat production/absorption are considered.

4. Effects of Brownian movement and thermophoresis are deemed.

FLOW ANALYSIS

The flow equations are based on the aforementioned assumptions.

$$\frac{\partial u}{\partial x}+\frac{\partial v}{\partial y}+\frac{\partial w}{\partial z}=0 \tag{1}$$

$$u\frac{\partial u}{\partial x}+v\frac{\partial u}{\partial y}+w\frac{\partial u}{\partial z}=\upsilon\left(1+\frac{1}{\beta}\right)\frac{\partial^2 u}{\partial z^2}-\frac{\sigma^* B_0^2}{\rho}u-\frac{\upsilon}{K}u \tag{2}$$

$$u\frac{\partial v}{\partial x}+v\frac{\partial v}{\partial y}+w\frac{\partial v}{\partial z}=\upsilon\left(1+\frac{1}{\beta}\right)\frac{\partial^2 v}{\partial z^2}-\frac{\sigma^* B_0^2}{\rho}v-\frac{\upsilon}{K}v \tag{3}$$

For the current study, suggested boundary conditions are

$$u=ax, v=by, \mathrm{w}=0 \qquad at \;\; z=0$$

$$u=0, \qquad v=0 \qquad \text{as} \quad z\to\infty \tag{4}$$

We now present the similarity transformation described below to transform the governing equations into a set of nonlinear ODE's:

$$\eta=z\sqrt{\frac{a}{\upsilon}}, u=axf'(\eta), v=ayg'(\eta), \mathrm{w}=-\sqrt{a\upsilon}\left(f(\eta)+g(\eta)\right) \tag{5}$$

We put eq. (5) in eqs. (1)- (3). Continuity Eq. (1) is automatically satisfied. We obtain coupled transformed nonlinear equations.

$$\left(1+\frac{1}{\beta}\right)f'''+\left(f+g\right)f''-f'^{2}-\left(M^{2}+\frac{1}{\lambda}\right)f'=0 \tag{6}$$

$$\left(1+\frac{1}{\beta}\right)g'''+\left(f+g\right)g''-g'^{2}-\left(M^{2}+\frac{1}{\lambda}\right)g'=0 \tag{7}$$

The modified boundary conditions are

$$f\left(0\right)=0, g\left(0\right)=0, f'\left(0\right)=1, \mathrm{g}'\left(0\right)=\alpha \qquad \text{at } \eta=0$$

$$f'\left(\infty\right)\to 0, \mathrm{g}'\left(\infty\right)\to 0 \qquad \text{at } \eta\to\infty \tag{8}$$

Here $\upsilon=\frac{\mu_B}{\rho}$ (kinematic viscosity coefficient), $\beta=\mu_B\sqrt{\frac{2\pi_p}{p_y}}$ (Casson fluid parameter), $M^2=\frac{\sigma^* B_0^2}{a\rho}$ (Hartmann number), $\lambda=\frac{Ka}{\upsilon}$ (Porosity parameter) and the Ratio parameter $\alpha=\frac{b}{a}$.

Shear stress coefficients (friction factors), which are physical variables of relevance to engineers, are given by:

$$C_{fx}=\frac{\tau_w x}{\rho u_w^2} \qquad C_{fy}=\frac{\tau_w y}{\rho u_w^2} \tag{9}$$

$$\mathrm{Re}_x^{-\frac{1}{2}}C_{fx}=\left(1+\frac{1}{\beta}\right)f''\left(0\right),$$

$$\mathrm{Re}_y^{-\frac{1}{2}}C_{fy}=\left(1+\frac{1}{\beta}\right)g''\left(0\right) \tag{10}$$

ANALYSIS OF HEAT TRANSFER

The energy equation for variable thermal conductivity, thermophoresis, Brownian motion and heat generation/absorption is given by

$$u\frac{\partial T}{\partial x}+v\frac{\partial T}{\partial y}+w\frac{\partial T}{\partial z}=\frac{1}{\rho c_p}\frac{\partial}{\partial z}\left(k^*(T)\frac{\partial T}{\partial z}\right)+\tau\left[D_B\left(\frac{\partial T}{\partial z}\right)\left(\frac{\partial C}{\partial z}\right)+\frac{D_T}{T_\infty}\left(\frac{\partial T}{\partial z}\right)^2\right]+\frac{Q}{\rho c_p}(T-T_\infty) \tag{11}$$

Where, T - fluid temperature, T_∞ - ambient temperature, T_w - fluid temperature of the wall, Q - the volumetric heat generation/absorption coefficient. Temperature dependent thermal conductivity is $k^*(T)=k_\infty(1+\varepsilon\theta)$.Where k_∞ is the fluid free stream conductivity and ε is a small parameter.

The energy equation's boundary conditions are provided by

$$T=T_w \quad at \quad z=0,\ T\to T_\infty \ \text{ as } z\to\infty \tag{12}$$

For the temperature variable, we define a dimensionless parameter of the form

$$\theta(\eta)=\frac{T-T_\infty}{T_w-T_\infty} \tag{13}$$

We put equation (13) is substituted into equation (11) to produce the following modified non-dimensional temperature equation:

$$(1+\varepsilon\theta)\theta''+\varepsilon\theta'^2+\Pr(f+g)\theta'+\Pr Nb\theta'\phi'+\Pr Nt\theta'^2+\Pr B\theta=0 \tag{14}$$

Where $\Pr=\frac{\upsilon}{\sigma}$ (Prandtl number), $B=\frac{Q}{a\rho c_p}$ (heat generation/absorption coefficient), $Nb=\frac{\tau D_B(C_w-C_\infty)}{\upsilon}$(Brownian motion parameter), and $Nt=\frac{\tau D_T(T_w-T_\infty)}{\upsilon T_\infty}$ (Thermophoresis parameter).

With the relevant boundary conditions

$$\theta(0)=1 \ \text{ at } \eta=0,\ \theta(\infty)\to 0 \quad \text{as } \eta\to\infty \tag{15}$$

The Nusselt number (Nu) for the present analysis is given

$$Nu_x = -\frac{xq_w}{k\left(T_w - T_\infty\right)}$$

$$\mathrm{Re}_x^{-\frac{1}{2}}\, Nu_x = -\theta'\left(0\right) \tag{16}$$

MASS TRANSFER ANALYSIS

The concentration equation with higher order chemical reaction is given by

$$u\frac{\partial C}{\partial x} + v\frac{\partial C}{\partial y} + w\frac{\partial C}{\partial z} = D_B\frac{\partial^2 C}{\partial z^2} + \frac{D_T}{T_\infty}\frac{\partial^2 T}{\partial z^2} - K_r\left(C - C_\infty\right)^n \tag{17}$$

Here C_w , C_∞ are near and far away the fluid concentration, D_B (diffusion coefficient), K_r - chemical reaction term.

The boundary conditions are written as

$$C = C_w \quad at \;\; z = 0,\; C \to C_\infty \;\; \text{as} \;\; z \to \infty \tag{18}$$

We define a concentration variable of the form

$$\phi\left(\eta\right) = \frac{C - C_\infty}{C_w - C_\infty} \tag{19}$$

By substituting equation (19) into equation (17) we get

$$\phi'' + Sc\left[\left(f + g\right)\phi'\right] + \frac{Nt}{Nb}\theta'' - ScK\phi^n = 0 \tag{20}$$

The boundary conditions are written as

$$\phi\left(0\right) = 1 \;\; \text{at} \;\; \eta = 0,\; \phi\left(\infty\right) \to 0 \quad \text{at} \;\; \eta \to \infty \tag{21}$$

Where $Sc = \frac{\upsilon}{D_B}$ (Schmidt Number), $K = \frac{k_r\left(C_w - C_\infty\right)^{n-1}}{a}$ (Chemical reaction parameter).

The local Sherwood number is given by:

$$Sh_x = -\frac{xj_w}{D\left(C_w - C_\infty\right)}$$

$$\mathrm{Re}_x^{-\frac{1}{2}} Sh_x = -\phi'(0) \tag{22}$$

Where $\mathrm{Re}_x = \frac{u_w x}{\upsilon}$ is definition of the Reynold's number.

3. METHOD OF SOLUTION

Since the leading gadget of equations are non-linear, to find the closed form of solutions it isn't always possible. Therefore, we are seeking a numerical solution of the governing model. Equations (6), (7), (14) and (20) along with the pertinent boundary conditions, equations (8), (15) and (21), are turned into a set of first order differential equations to solve the current issue, and the solution is described using the boundary value problem solver bvp4c in MATLAB. This programme implements a collocation strategy under preferred nonlinear, two-point boundary conditions g (y(a), y(b), q) to handle boundary value issues for ordinary differential equations in the frame y f (x, y, q), [a, b]. Here, the vector q contains unknowable parameters. In the majority of unique systems, boundary value issues (BVPs) appear. With bvp4c, pretty much any BVP may be designed for a solution with bvp4c.

4. RESULTS AND DISCUSSION

This subdivision investigates how non-dimensional velocity, temperature, and concentration distributions are affected by flow controlling parameters. With computational solutions, it is possible to access the main characteristics of the flow bearing. Using graphs and tables, numerical results are presented in the form of velocity, temperature, and concentration as well as the friction factor, local heat transfer rates, and mass transfer rates. We have discussed the variations of the following parameters on the flow fields: the ratio parameter(α), thermophoresis parameter (Nt), brownian motion parameter (Nb), order of chemical reaction (n), schmidt number (Sc), chemical reaction parameter (K),Thermal conductivity parameter (ε), Heat generation/absorption parameter(B) and Prandtl Number (Pr) on the flow fields. We prescribed the values of $Nb = 1.0, M = 0.6, \varepsilon = 0.7, \beta = 1.5, \mathrm{Pr} = 0.9, B = 0.4, \lambda = 2.0, K = 0.3, n = 1, \alpha = 1.5, Nt = 0.5, Sc = 0.6$ for computation purposes. In the graphs, f′(η), g'(η), θ(η), and φ(η) establish the flow velocity, temperature and concentration distributions.

Velocity profiles

The outputs of the Ratio parameter (α) on the gradient of velocity fluid profiles are shown in Figs. 1 and 2. We can see that the boundary layer thickness goes down the velocity

along the x axis. Figure 2 displays velocity profiles for the y direction at different **α** values. The thickness of the momentum and velocity boundary layers is shown in this picture to be a function of α. The issue is reduced to flow near the two-dimensional stagnation point when the parameter α = 0. Compared to its component in the y-direction, the effect of ratio parameter on velocity component in x- direction is significantly less pronounced. The velocity in the y-direction increases with an increase in α, which indicates that the velocity in the y-direction exceeds the velocity in the x-direction.

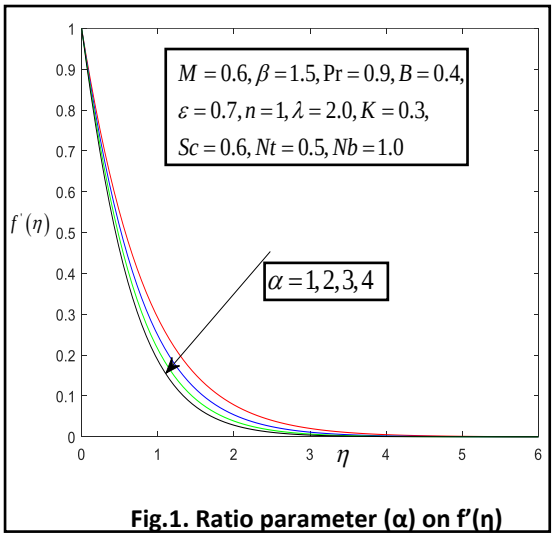

Fig.1. Ratio parameter (α) on f'(η)

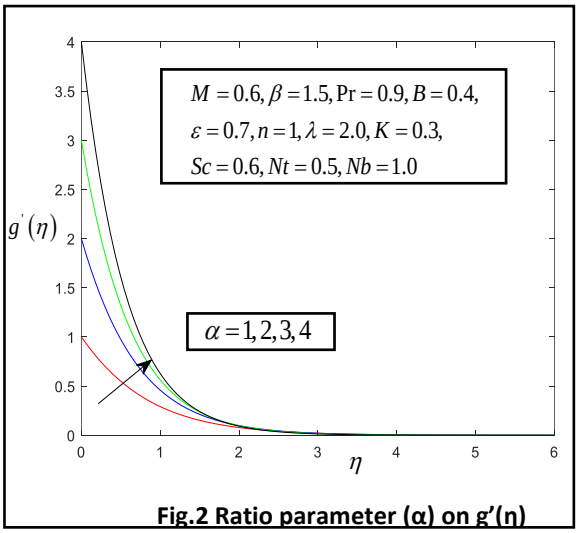

Fig.2 Ratio parameter (α) on g'(η)

Temperature profiles

Figures. 3- 6 highlight how the gradient of temperature profiles are influenced by the Ratio parameter (α), Thermophoresis parameter (Nt), Brownian motion parameter (Nb), and thermal conductivity parameter (**ε**). It is important to note that the interaction between the temperature profile and the Ratio parameter (α) decreases. For the parameters Nt, Nb, and ε, however, the opposite tendency is seen. Figure 3 shows that as the thermophoresis parameter Nt increases, the temperature profile becomes more intense. Temperature gradient that causes particles to travel from a hot to a cool location, enlarge the thickness of the thermal boundary layer. As the Brownian motion parameter Nb is increased in Fig. 5, the temperature field and thermal boundary layer thickness both increase. Collisions between fluid particles will grow as Nb increases. As a result, more heat will be produced. According to Fig. 6, the presence of varied conductivity pushes the temperature upward across the fluid layers as is to be expected because an increase in the fluid's thermal conductivity causes the fluid to heat up more, resulting in a higher temperature.

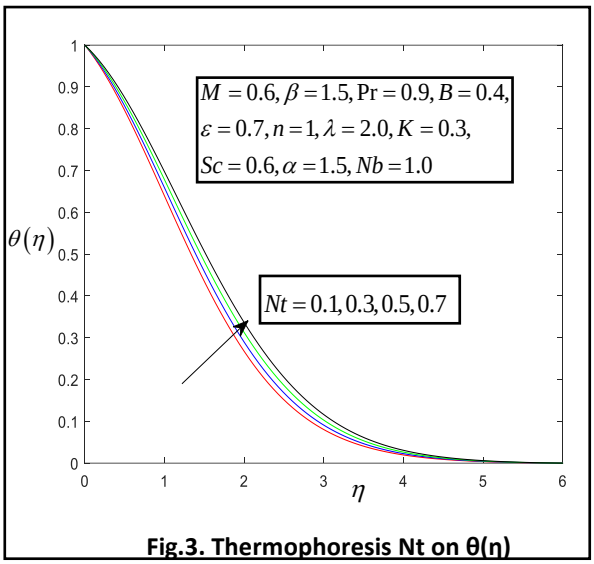

Fig.3. Thermophoresis Nt on θ(η)

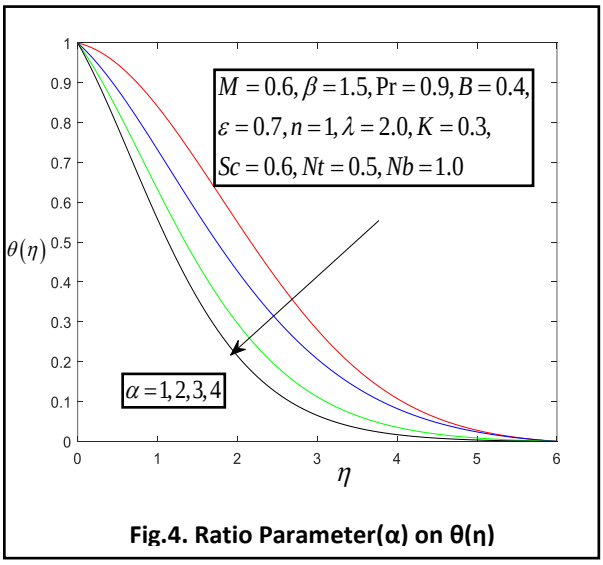

Fig.4. Ratio Parameter(α) on θ(η)

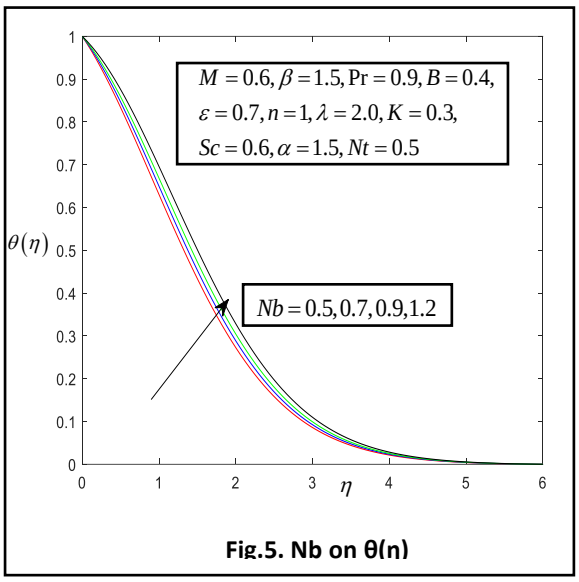

Fig.5. Nb on θ(η)

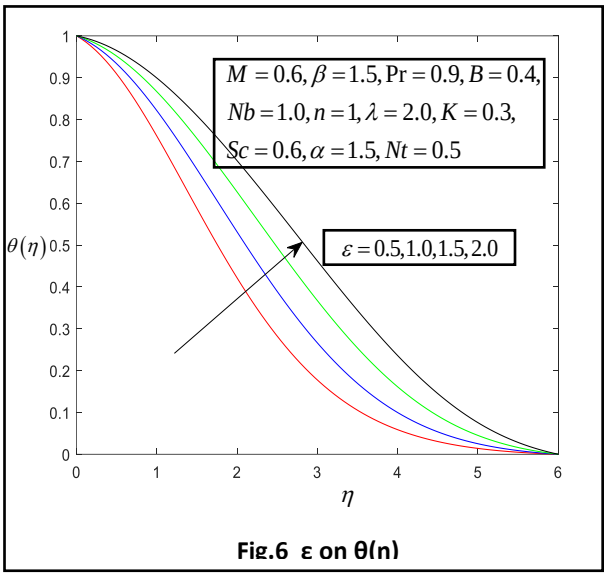

Fig.6 ε on θ(η)

Concentration profiles

Figs. 7–12 illustrate the effects of the ratio parameter (α), the thermophoresis parameter (Nt), the Brownian motion parameter (Nb), the order of the chemical reaction (n), the Schmidt Number (Sc), and the chemical reaction parameter (K) on concentration profiles. Thermophoresis parameter and greater chemical reaction order (n) are shown to increase the concentration profile (Nt). According to Fig. 7, as the thermophoresis parameter Nt increases, the concentration field and thickness of the solid boundary layer both get better. Physically, as the thermophoresis parameter increases, the pressure increases. Hence, there will be more heat transmission, which improves the diffusion effects. The Ratio parameter (), Brownian motion parameter (Nb), Schmidt Number (Sc), and Chemical reaction parameter, however, all show

the opposite trend (K). It is noted in Fig. 9 that the concentration field represents the Brownian motion parameter (Nb) decaying behaviour. Collisions between fluid particles will increase as Brownian motion does. As a result, a little quantity of mass is shifted, which causes the concentration distribution to decline. Fig. 11 shows how the Schmidt number affects the concentration profile. It is expected that increasing the Schmidt number (Sc) will result in a decline in the concentration profile. It is anticipated that the concentration profiles of the flow field will be more slowed down by the heavier diffusing species. To examine the impact of the chemical reaction parameter (K) on the concentration profile, Fig. 12 is presented. The graph clearly shows that a rise in the chemical reaction parameter suppresses the concentration field and thickness of the solid boundary layer. This is due to the fact that a fall in concentration profile can be seen when an implement is used in the interfacial mass transfer.

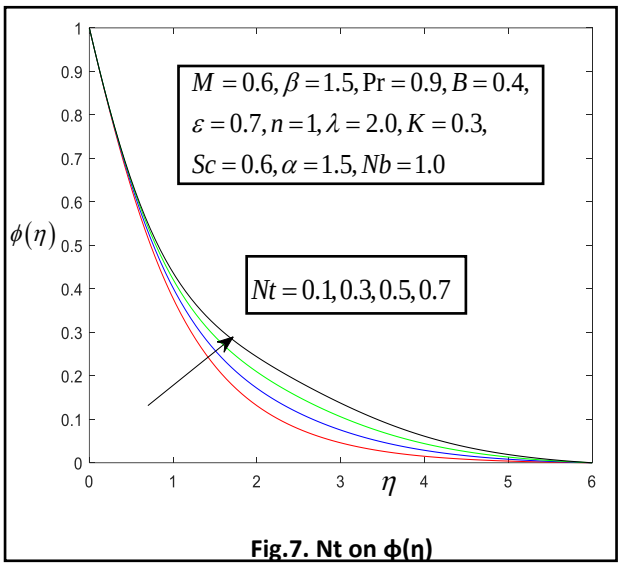

Fig.7. Nt on ϕ(η)

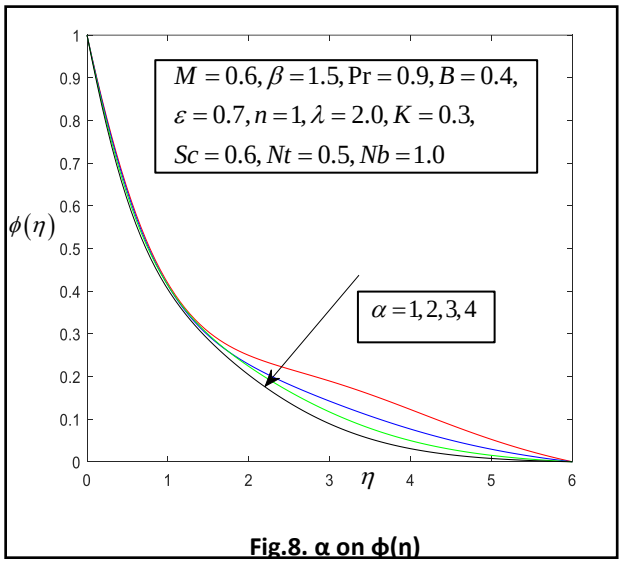

Fig.8. α on ϕ(η)

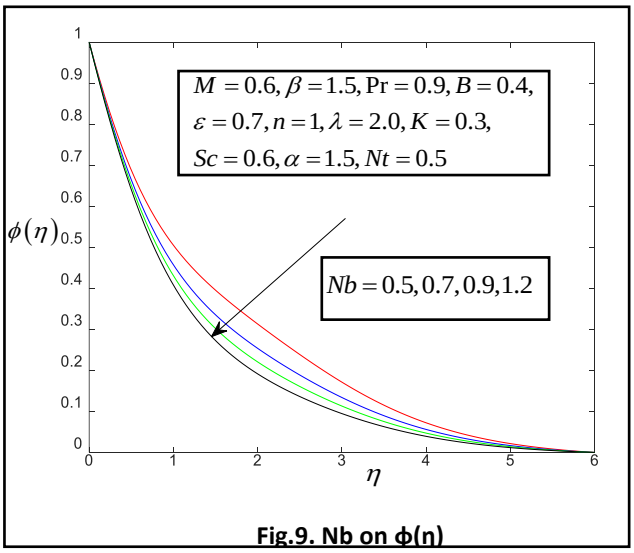

Fig.9. Nb on ϕ(η)

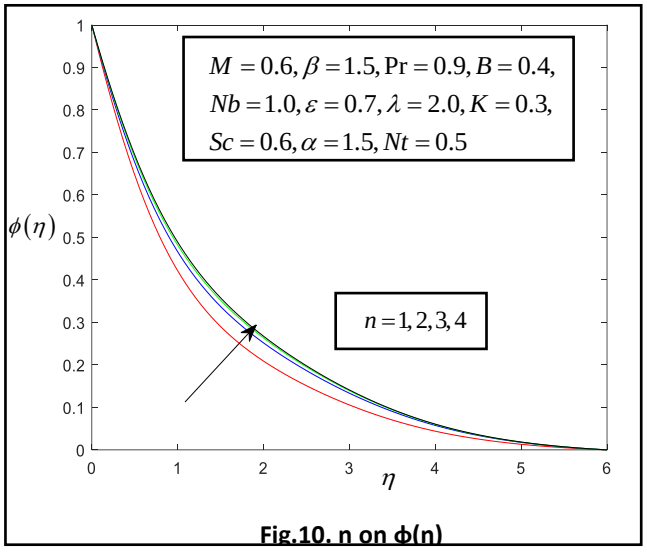

Fig.10. n on ϕ(η)

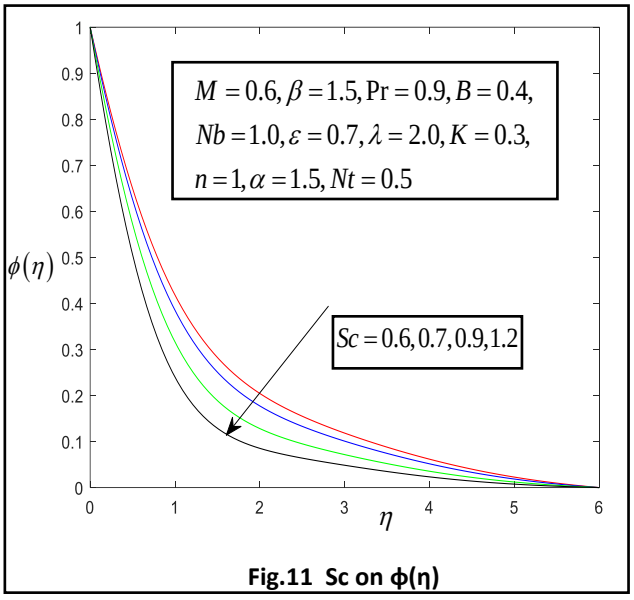

Fig.11 Sc on ϕ(η)

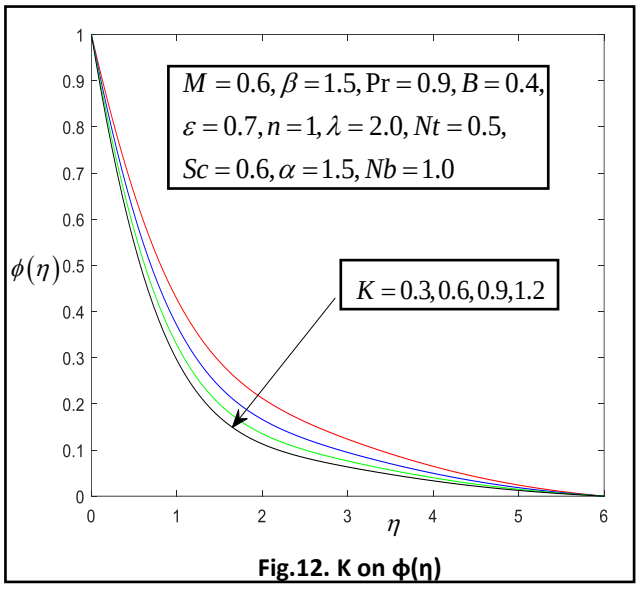

Fig.12. K on ϕ(η)

Rate of Heat Transfer and Rate of Mass transfer profiles

Analysis of the local Nusselt and Sherwood number profiles shown in Fig.13–18 for the thermal conductivity parameter (**ε** Vs B), heat generation/absorption parameter (B Vs Nt), chemical reaction parameter (K Vs Sc), chemical reaction order (n Vs Sc), and Prandtl number (Pr Vs B). With increasing trends in Thermal conductivity parameter (**ε** Vs B), Heat generation/absorption parameter (B Vs Nt), and Prandtl number, the rate of heat transfer constantly decreases (Pr Vs B). It should be noted that sluggish cooling results from reduced heat transfer from the surface, which has an adverse effect on the surface's mechanical qualities like stiffness, strength, and hardness. Also, we have seen that improving the local Sherwood

number profiles results from increasing the values of the chemical reaction parameter (K Vs Sc), heat generation/absorption parameter (B Vs Nt), and order of chemical reaction (n Vs Sc).

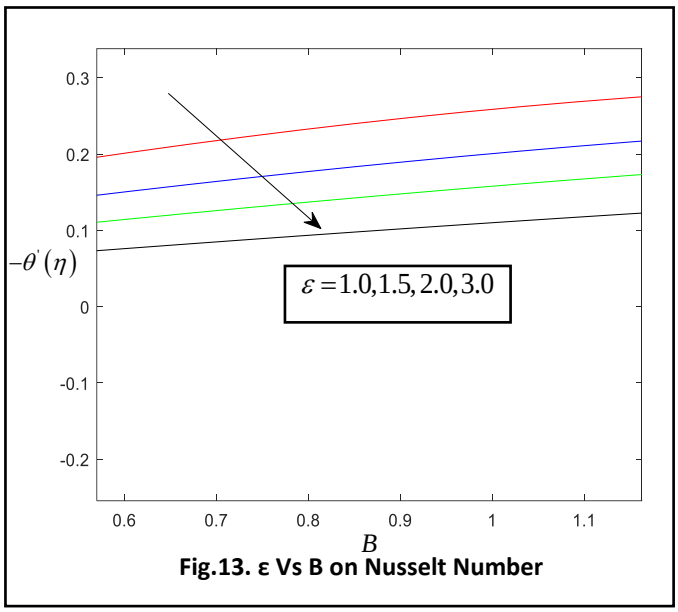

Fig.13. ε Vs B on Nusselt Number

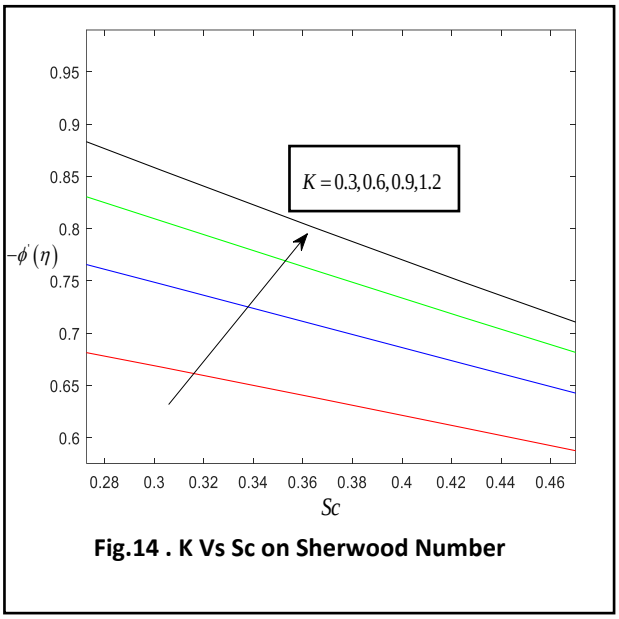

Fig.14 . K Vs Sc on Sherwood Number

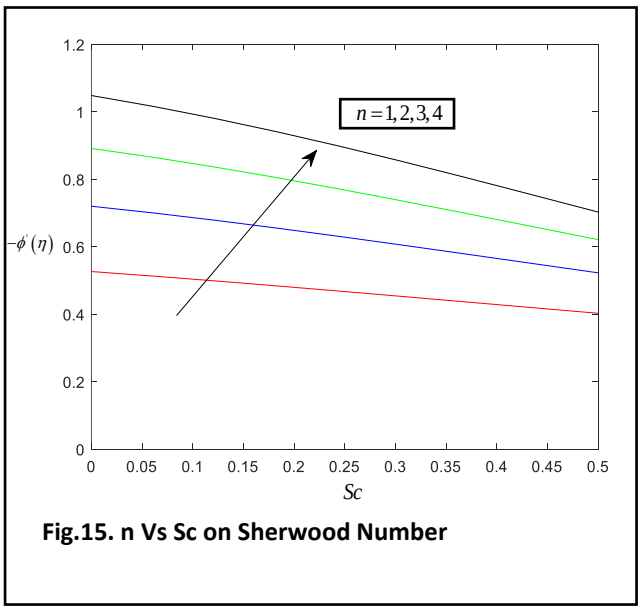

Fig.15. n Vs Sc on Sherwood Number

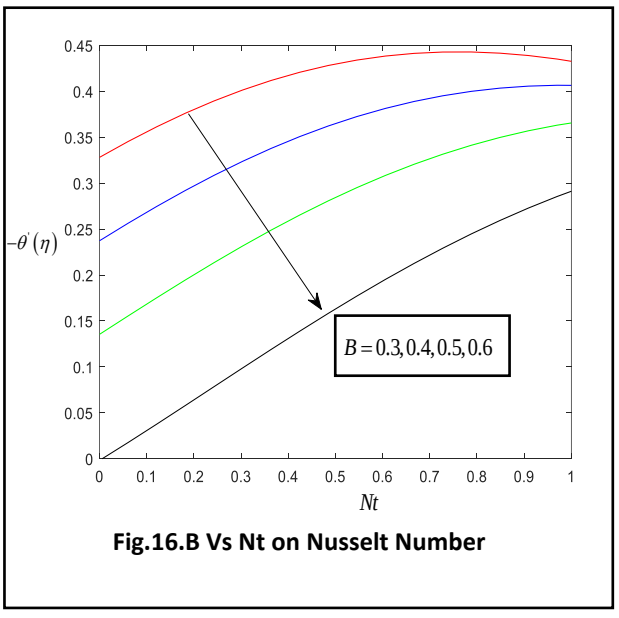

Fig.16.B Vs Nt on Nusselt Number

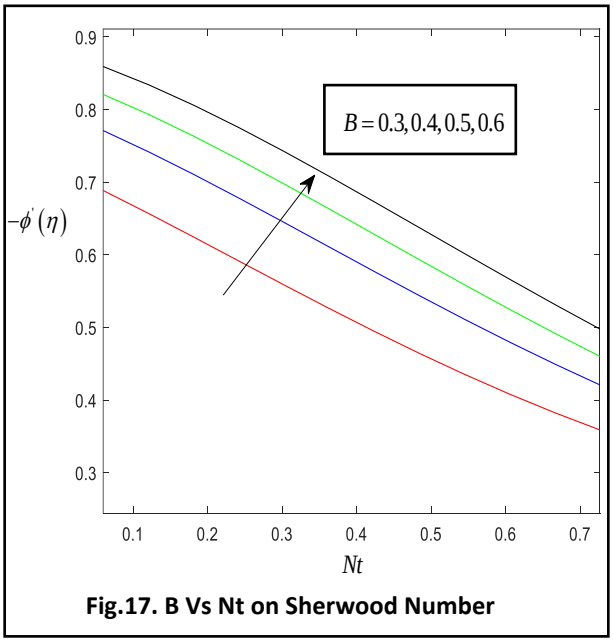

Fig.17. B Vs Nt on Sherwood Number

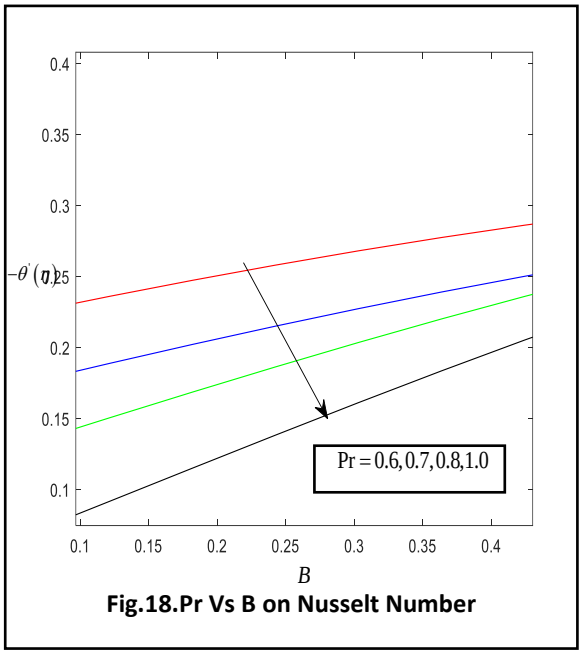

Fig.18.Pr Vs B on Nusselt Number

5. CONCLUSIONS

This research can be helpful in building processes for automated production and based on viscosity nature. The nature of magnetohydrodynamic heat and mass transmission is examined theoretically. Casson fluid with thermophoresis and Brownian moment effects moving towards a stretching surface. The model includes effects from higher order chemical reactions and variable heat conductivity. Using MATLAB's bvp4c approach, the governing equation of the flow is converted utilising fitting similarity variables. The following numerical observations are made:

Compared to its component in the y-direction, the effect of α on velocity in the x-direction is significantly less pronounced. The velocity in the y-direction increases with a drop in the x-component because an increase in indicates that the velocity in the y-direction exceeds the velocity in the x-direction.

With the help of the Ratio parameter (α), the interaction of the temperature profile reduces. For the parameters Nt, Nb, and, however, the opposite tendency is seen.

Thermophoresis parameter and higher order chemical reaction (n) improve concentration profile (Nt). The Ratio parameter (α), Brownian motion parameter (Nb), Schmidt Number (Sc), and Chemical reaction parameter, however, all show the opposite trend (K).

With increasing trends in Thermal conductivity parameter (**ε** Vs B), Heat generation/absorption parameter (B Vs Nt), and Prandtl number, the rate of heat transfer constantly decreases (Pr Vs B).

The local Sherwood number profiles are improved by increasing the values of the chemical reaction parameter (K Vs Sc), the heat generation/absorption parameter (B Vs Nt), and the order of the chemical reaction (n Vs Sc).

Table 1. Values of Skin-friction, Nusselt and Sherwood number for various values of governing parameters.

Parameter	Values	$-\left(1+\frac{1}{\beta}\right)f''(0)$	$-\left(1+\frac{1}{\beta}\right)g''(0)$	$-\theta'(0)$	$-\phi'(0)$
Nt	0.2	2.021023	0.924717	0.12866	0.77958
	0.3	2.021024	0.924717	0.11458	0.85011
Nb	0.2	2.021023	0.924717	0.12860	0.71858
	0.4	2.021024	0.924717	0.10202	0.71311
Pr	1.0	2.021023	0.924717	0.17512	0.70901
	1.5	2.021024	0.924717	0.31514	0.62347
K	0.3	2.021023	0.924717	0.14273	0.72881
	0.6	2.021024	0.924717	0.14281	0.87901
Sc	0.9	2.021023	0.924717	0.14276	0.92161
	1.2	2.021024	0.924717	0.14300	1.08701
N	3.0	2.021023	0.924717	0.14291	0.61454
	5.0	2.021024	0.924717	0.14283	0.58614

REFERENCES

[1] Abdela, Y., and Shankar, B., The Influence of Non-Uniform Heat Source and Thermal Radiation on the MHD Stagnation Point Flow of Maxwell Nanofluid Over a Linear Stretching Surface, International Journal of Mathematics Trends and Technology (IJMTT), 2018, Vol.56, pp.271-288.

[2] Alreshidi, N.A., Shah, Z., Dawar, A., Kumam, P., Shutaywi, M., and Watthayu, W., Brownian Motion and Thermophoresis Effects on MHD Three Dimensional Nanofluid Flow with Slip Conditions and Joule Dissipation Due to Porous Rotating Disk, Molecules,2020, Vol.25(3), pp.1-20, doi:10.3390/molecules25030729.

[3] Animasaun, I.L., Casson Fluid Flow with Variable Viscosity and Thermal Conductivity along Exponentially Stretching Sheet Embedded in a Thermally Stratified Medium with Exponentially Heat Generation, Journal of Heat and Mass Transfer Research ,2015, Vol.2, pp.63-78.

[4] Arshad, M., Hussain, A., Hassan, A., Haider, Q., Ibrahim, A.H., Alqurashi, M.S., Almaliki, A.H., and Abdussattar, A., Thermophoresis and Brownian Effect for Chemically Reacting Magneto-Hydrodynamic Nanofluid Flow across an Exponentially Stretching Sheet, Energies, 2022, Vol.15, pp.1-15, https://doi.org/10.3390/en15010143.

[5] Falana, A., Ojewale, O. A., and Adeboje, T. B., Effect of Brownian Motion and Thermophoresis on a Nonlinearly Stretching Permeable Sheet in a Nanofluid, Advances in Nanoparticles, Vol.5, pp.123-134, http://dx.doi.org/10.4236/anp.2016.51014.

[6] Gopal, D., and Kishan, N., Brownian Motion and Thermophoresis Effects on Casson Nanofluid Over a Chemically Reacting Stretching Sheet with Inclined Magnetic Field, AAM: Intern. J., 2019, Vol.4, pp.106-116.

[7] Gopal, D., Saleem, S., Jagadha, S., Ahmad, F., Othaman Almatroud, A., and Kishan, N., Numerical analysis of higher order chemical reaction on electrically MHD nanofluid under influence of viscous dissipation, Alexandria Engineering Journal, Vol.60, Issue 1, 2021, pp. 1861-1871.

[8] Hari Krishna, Y., Reddy, G.V.R., and Makinde, O.D., Chemical Reaction Effect on MHD Flow of Casson Fluid with Porous Stretching Sheet, Defect and Diffusion Forum, 2018, Vol. 389, pp. 100-109, DOI: 10.4028/www.scientific.net/DDF.389.100.

[9] Ismail, H.N., Abdel-Wahed, M.S., and Omama, M., Effect of Variable thermal conductivity on the MHD boundary layer of Casson-Nanofluid over a Moving plate with variable thickness, Thermal Science, 2019, Vol. 25, pp.1-17, DOI:10.2298/TSCI190324293I.

[10] Jana, S., and Das, K., Influence of variable fluid properties, Thermal radiation and chemical reaction on MHD slip flow over a flat plate, Italian journal of pure and applied mathematics, 2015, Vol.34, pp.29-44.

[11] Jangid, S., Mehta, R., Mehta, T., and Sushila., Mathematical modelling of steady MHD Casson fluid flow with stretching porous walls in existence of radiation, chemical reaction, and thermal diffusion effect, Mathematical Methods in Applied Sciences., 2021, Vol.2021, pp.1–20, doi:10.1002/mma.7732.

[12] Khan, Z., Rasheed, H.U., Khan, I., Abu-Zinadah, H., and Aldahlan, M.A., Mathematical Simulation of Casson MHD Flow through a Permeable Moving Wedge with Nonlinear Chemical Reaction and Nonlinear Thermal Radiation, Materials, 2022, Vol.15, pp.1-16, https://doi.org/10.3390/ma15030747.

[13] Kumar, S.G., Varma, S.V.K., Prasad, P.D., Raju, C.S.K., Makinde, O.D., and Sharma, R., MHD reacting and radiating 3-D flow of Maxwell fluid past a stretching sheet with heat source/sink and Soret effects in a porous medium, Defect and Diffusion Forum, 2018, Vol.387, pp.145-156.

[14] Loganathan, P., and Deepa, K., Heat and mass transfer analysis of Casson fluid flow on a permeable Riga-plate, Indian Journal of Pure & Applied Physics, 2020, Vol. 58, pp. 79-86.

[15] M.V. Reddy., Pallavarapu, L., Vajravelu, K., A Comparative Study of MHD Non-Newtonian fluid flows with the effects of Chemical reaction and Radiation over a stretching sheet, Computational Thermal Sciences: An International Journal, 2021, Volume 13, pp.17-29, 10.1615/ComputThermalScien.2021037094.

[16] Majeed, A., Zubair, M., Khan, A., Muhammad, T., and Alqarni, M.S., Significance of Thermophoretic and Brownian Motion on MHD Nanofluids Flow towards a Circular Cylinder under the Inspiration of Multiple Slips: An Industrial Application, Mathematical Problems in Engineering, 2021, Vol. 2021, pp.1-14, https://doi.org/10.1155/2021/8634185.

[17] Makinde, O.D., MHD mixed-convection interaction with thermal radiation and n^{th} order chemical reaction past a vertical porous plate embedded in a porous medium, Chemical Engineering Communications, 2011, Vol.198, pp.590-608.

[18] Makkar, V., Poply, V., Goyal, R., and Sharma, N., Numerical investigation of MHD Casson Nanofluid flow towards a Non-linear stretching sheet in presence of double diffusive effects along with viscous and Ohmic dissipation, Journal of Thermal Engineering, 2021, Vol. 7, No. 2, pp. 1-17.

[19] Mittal, A.S., and Patel, H.R., Influence of thermophoresis and Brownian motion on mixed convection two dimensional MHD Casson fluid flow with non-linear radiation and heat generation, Physica A: Statistical Mechanics and its Applications, 2020, Vol.537, pp.1-12, https://doi.org/10.1016/j.physa.2019.122710.

[20] Mondal, H., Almakki, M., Sibanda, P., Dual solutions for three-dimensional Magnetohydrodynamic nanofluid flow with entropy generation, Journal of Computational Design and Engineering, 2019, Vol. 6, pp. 657–665.

[21] Radha, G., Reddy, N.B., and Gangadhar, K., Slip Flow of Casson Fluid with Variable Thermo Physical Properties along exponentially Stretching Sheet under Convective Heating, International Journal of Mechanics and Solids, 2017, Vol.12, pp. 235-256.

[22] Raju, C.S.K., Sandeep, N., Ali, M.E., and Nuhait, A.O., Heat and Mass Trasnfer in 3D MHD Williamson-Casson fluids flow over a stretching surface with non-uniform heat source/sink, Thermal Science, 2019, Vol.23, pp.281-293.

[23] Ramadevi, B., Ramana Reddy, J.V., Sugunamma, V., Influence of Thermo diffusion on Time Dependent Casson Fluid Flow past a Wavy Surface, International Journal of Mathematical, Engineering and Management Sciences, 2018, Vol. 3, No. 4, pp.472–490, https://dx.doi.org/10.33889/IJMEMS.2018.3.4-034.

[24] Rasheed, H.U., Islam, S., Helmi, M.M., Alsallami, S.A.M., Khan, Z., and Khan, I., An Analytical study of internal heating and chemical reaction effects on MHD flow of Nanofluid with Convective conditions, Crystals, 2021, Vol.11, pp.1-21.

[25] Reddy, S., Naikoti, K., and Rashidi, M.M., MHD flow and heat transfer characteristics of Williamson nanofluid over a stretching sheet with variable thickness and variable thermal conductivity, Transactions of A. Razmadze Mathematical Institute, 2017, Vol. 171, pp.195-211.

[26] Sarojamma, G., Sreelakshmi, K., P.K. Jyothi, P.V. Satya Narayana, Influence of Homogeneous and Heterogeneous Chemical Reactions and Variable Thermal Conductivity on

the MHD Maxwell Fluid Flow due to a Surface of Variable Thickness, Defect and Diffusion Forum, 2020, Vol.401, pp.148–163, DOI: 10.4028/www.scientific.net/ddf.401.148.

[27] Sarojamma, G., Vasundhara, B., and Vendabai, K., MHD Casson Fluid Flow, Heat and Mass Transfer in a Vertical Channel with Stretching Walls, International Journal of Scientific and Innovative Mathematical Research (IJSIMR), 2014, Vol. 2, Issue 10, pp.800-810.

[28] Senapati, M., Kharabela, S., and Sampad Kumar, P., Numerical analysis of three-dimensional MHD flow of Casson nanofluid past an exponentially stretching sheet, Karbala International Journal of Modern Science, 2020, Vol. 6, pp.1-12, https://doi.org/10.33640/2405-609X.1462.

[29] Sivakumar, N., and Rushi Kumar, B., Variable conductivity and heat source or sink on MHD unsteady radiated partial slip flow over a sheet with chemical reaction, AIP Conference Proceedings, 2020, Vol.2020, pp.1-10, https://doi.org/10.1063/5.0025244 .

[30] Swain, K., Parida, S.K., and Dash, G.C., Higher Order Chemical Reaction on MHD Nanofluid Flow with Slip Boundary Conditions: A Numerical Approach, Mathematical Modelling of Engineering Problems, Vol. 6, 2019, pp. 293-299.

[31] Tufail, M.Z., Zaib, F., Symmetry analysis of MHD Casson fluid flow for heat and mass transfer near a stagnation point over a linearly stretching sheet with variable viscosity and thermal conductivity, 2021, Vol.50, pp. 5418-5438, https://doi.org/10.1002/htj.22131.

[32] Ullah, I., Shafie, S., Khan, I., and Hsiao, K.L., Brownian diffusion and thermophoresis mechanisms in Casson fluid over a moving wedge, Results in Physics, 2018, Vol. 9, pp.183-194.